FULL PAPER

Understanding the Host–Guest Interaction Between Responsive Core-Crosslinked Hybrid Nanoparticles of Hyperbranched Poly(ether amine) and Dyes: The Selective Adsorption and Smart Separation of Dyes in Water

Rui Wang, Bing Yu, Xuesong Jiang, and Jie Yin*

The host–guest interaction between polymer nanoparticles and guest molecules plays a key role in fields such as controlled drug delivery, separation, and nanosensors. To understand this host–guest interaction, a series of hybrid polymer nanoparticles ($SiO_{1.5}$-hPEA NPs) are designed and prepared based on hyperbranched poly(ether amine) (hPEA) with the different hydrophobicity and functional groups. Their adsorption behavior to twelve hydrophilic dyes in aqueous solution is studied. The core-crosslinked hybrid nanoparticles ($SiO_{1.5}$-hPEA NPs) are prepared by direct dispersion of hPEA containing trimethoxysilyl moieties (TMS-hPEA) in aqueous solution, which exhibit sharp multiresponse to temperature, pH, and ionic strength in aqueous solution. The effect of molecular structure of TMS-hPEA on the host–guest interaction between $SiO_{1.5}$-hPEA NPs and hydrophilic dyes is investigated in detail. The obtained $SiO_{1.5}$-hPEA NPs interact selectively with different hydrophilic dyes in aqueous solution. The distribution coefficient (*K*) for partitioning of dyes between $SiO_{1.5}$-hPEA NPs and water is proposed to define the strength of the host-guest interaction between the nanoparticles and dyes. *K* increases with the increasing hydrophobicity of the hPEA backbone regardless of their charge states of $SiO_{1.5}$-hPEA NPs and dyes. A methodology is demonstrated for the smart separation of a mixture of dyes in water using $SiO_{1.5}$-hPEA NPs.

1. Introduction

Core/shell polymer nanoparticles have been regarded as interesting candidates for application in supramolecular host–guest chemistry because of their unique properties.[1–4] Polymeric micelles with hydrophobic core surrounded by hydrophilic shell could encapsulate apolar guests in polar solvents and show great potential of polymer particles as drug carriers.[5–9] Inverse micelles with hydrophilic core surrounded by hydrophobic shell could encapsulate and transfer polar guests,[2,4,10–14] such as the dyes rose bengal, rhodamine, methyl orange, from polar solution to apolar solvent and have great potential in decoloration and removal of dyes from industries waste based on textiles, paper, plastics, leather, food, and cosmetic. During these dye processes, the release of colored dyes into the ecosystem is a dramatic source of pollution and of perturbation to aquatic life.[15,16] The adsorption on porous carbons (mainly activated carbons) is the most widely studied method of dye removal and decoloration.[17–23] However, its use is still limited by high operating costs. The application of the inverted micelles in liquid–liquid extraction of dyes is another promising method for efficient waste water treatment.[24] Frey and Stiriba reported core/shell amphiphilic hyperbranched polyglycerol (HPG) or hyperbranched polyethyleneimine (HPEI) for encapsulating and extracting water-soluble dyes from aqueous solution into organic media such as chloroform.[25–28] In most of these cases, organic solvents must be used as transferring solvent, which is essential for the dye removal. In some cases, the release of encapsulated guest molecules could be achieved by changing the environmental conditions, such as pH, to degrade the host units.[9,11,29] To the best of our knowledge, however, no stimuli-triggered dye removal has been addressed directly in aqueous solution. The responsive polymer nanoparticles provide the possibility to remove the hydrophilic dyes from water directly.

Another important issue related to host–guest interaction between polymer nanoparticles and guest molecules is selectivity. Haag and Wan reported core/shell polymer architectures based on polyamine or polyglycerol as supramolecular host for transferring various guest molecules from the aqueous phase to the organic phase with selectivity, suggesting selective molecular recognition.[30–33] Thayumanavan also investigated the application of several amphiphilic polymers in selective binding and extraction of hydrophilic dyes.[34–37] These polymer architectures with selective binding of guest molecules were usually based on the unimolecular micelles or non-crosslinked polymer micelles.

R. Wang, B. Yu, Prof. X. S. Jiang, Prof. J. Yin
School of Chemistry & Chemical Engineering
State Key Laboratory for Metal Matrix Composite Materials
Shanghai Jiao Tong University
Shanghai 200240, P. R. China
E-mail: ponygle@sjtu.edu.cn

DOI: 10.1002/adfm.201102902

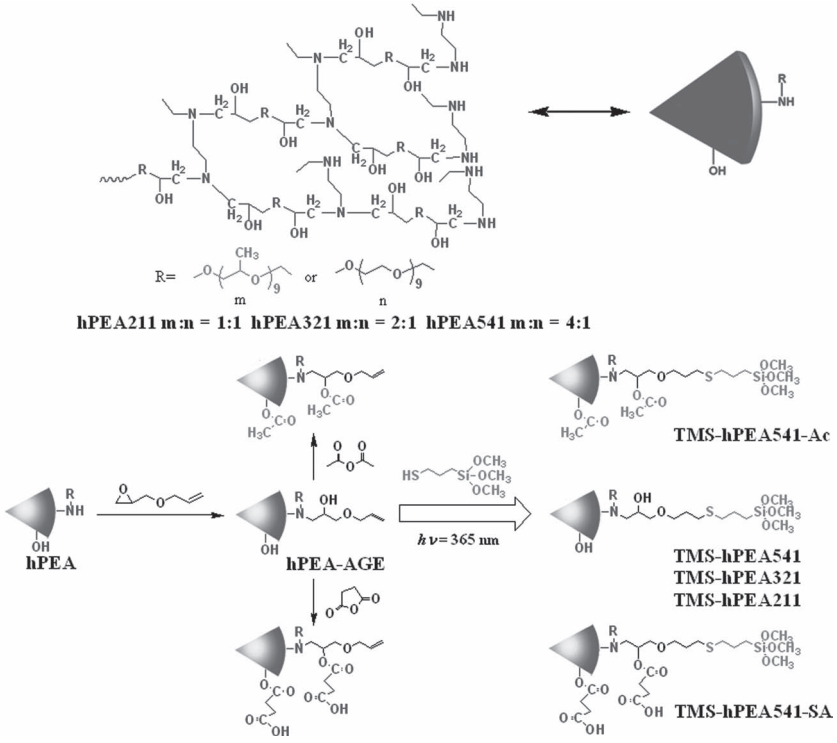

Scheme 1. Synthesis process for TMS-hPEAs.

Unlike the described polymer micelles, we recently found that the responsive core-crosslinked organosilica hybrid nanoparticles of poly(ether amine) with selective adsorption of the hydrophilic dyes in water and the separation of the mixed dyes can be addressed directly in aqueous solution. This was controlled by temperature.[38] Due to their stability and versatile structure, core-crosslinked organosilica hybrid nanoparticles allow for systematic investigation of host–guest interactions under various conditions.[39] The selective adsorption of guest molecules gives the organosilica hybrid nanoparticles of poly(ether amine) potential in separation, catalytic chemistry, and chemical and biological sensing. The complex formation between the host hybrid nanoparticles and the guest hydrophilic dyes depends on many parameters, including topological trapping, solvation effects, hydrogen bond formation, and hydrophobic and electrostatic interactions.[30,32] Therefore, fundamental understanding of the host–guest interaction between hybrid nanoparticles of poly(ether amine) and the hydrophilic dyes is necessary before their application. Investigation based on hyperbranched polymers is promising due to their high functionality.[40–42]

Here, we design and prepare a series of core-crosslinked hybrid nanoparticles based on hyperbranched poly(ether amine) ($SiO_{1.5}$-hPEA NPs) with different hydrophobicity and functional groups and then systematically investigate the host–guest interaction between these hybrid nanoparticles and twelve hydrophilic dyes in aqueous solution. The distribution coefficient (*K*) for partitioning of dyes between $SiO_{1.5}$-hPEA NPs and water is proposed to quantitate the host–guest interaction between $SiO_{1.5}$-hPEA NPs and dyes. Particular attention is paid to the effect of the molecular parameters of $SiO_{1.5}$-hPEA NPs on the distribution coefficient (*K*). The large difference in *K* for different dyes indicates that $SiO_{1.5}$-hPEA NPs selectively adsorb dyes. By using $SiO_{1.5}$-hPEA NPs, finally, we demonstrated an approach to separate dye from their mixture based on the established *K*.

2. Results and Discussion

2.1. Design, Preparation, and Characterization of $SiO_{1.5}$-hPEA NPs

Trimethoxysilane groups containing hyperbranched poly(ether amine)s (TMS-hPEAs), whose structure and synthesis processes are shown in **Scheme 1**, were used to fabricate the core-crosslinked hybrid nanoparticles. Because of the ability to be functionalized sequentially, different functional groups can be easily grafted to the backbone of hPEAs, which were synthesized according to the previous report.[43] Therefore, variations of the molecular structure are helpful to understand the effect of the molecular parameters of $SiO_{1.5}$-hPEA NPs on the host–guest interaction. For example, we introduced the carboxyl groups into the backbone of hPEAs to check the effect of charge state of $SiO_{1.5}$-hPEA NPs. The structure of the obtained TMS-hPEA was confirmed by Fourier transform infrared (FTIR) spectroscopy and ^{1}H NMR spectroscopy, the results of which are included in the Supporting Information.

Due to their amphiphilic property, TMS-hPEAs could be dispersed directly into water and self-assemble into micelles with hydrophobic poly(propylene oxide) (PPO) and TMS as the core and hydrophilic poly (ethylene oxide) (PEO) as the shell. After hydrolysis and condensation catalyzed by amine groups in the molecules, core-crosslinked hybrid particles were obtained. The process for formation of $SiO_{1.5}$-hPEAs is illustrated in **Scheme 2**. The size distribution of the obtained $SiO_{1.5}$-hPEAs was revealed by dynamic light scattering (DLS; **Figure 1**). In aqueous solution, $SiO_{1.5}$-hPEAs form well-dispersed nanoparticles (NPs) with diameters ranging from 10 to 20 nm and low polydispersity indexes (PDI) of around 0.35. $SiO_{1.5}$-hPEA541

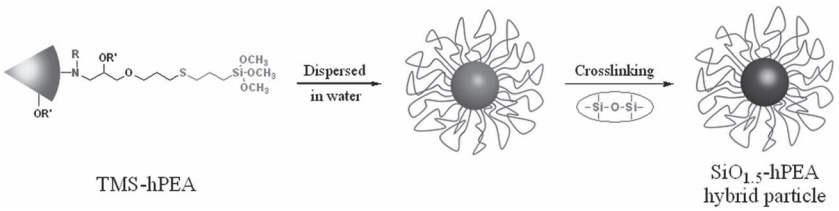

Scheme 2. Preparation of $SiO_{1.5}$-hPEAs hybrid nanoparticles in water.

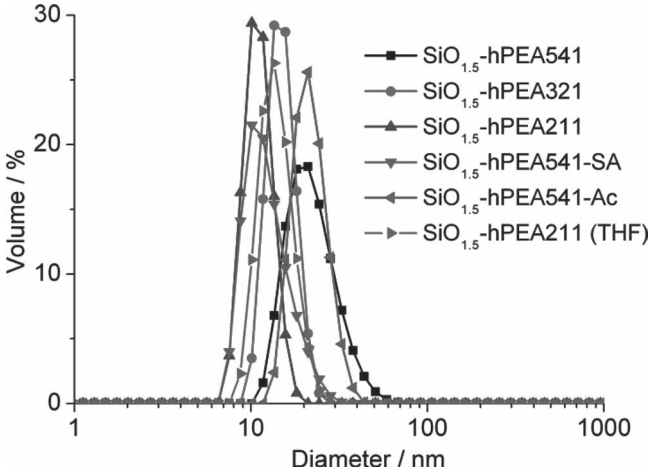

Figure 1. Volume-weighted size distribution of $SiO_{1.5}$-hPEA NPs in aqueous and THF solution (concentration c = 1 g L^{-1}) obtained using DLS at room temperature.

and $SiO_{1.5}$-hPEA541-Ac have larger particles because of their more hydrophobic cores. The formation of crosslinked core was proven by the DLS of $SiO_{1.5}$-hPEA particles in tetrahydrofuran (THF). As shown in Figure 1, $SiO_{1.5}$-hPEA211 particles do not disassemble in THF and the particle size increased slightly, which might be due to swelling of the crosslinked core in the good solvent. The increased stability of $SiO_{1.5}$-hPEA provides reinforcement to the particle existence and broadens its potential application.[44] The morphology of the obtained hybrid nanoparticles was also revealed using transmission electron microscopy (TEM, Supporting Information Figure S3). Compared with particles in aqueous solution, the size of $SiO_{1.5}$-hPEA211 in THF is larger, which in good agreement with DLS results.

The responsive aggregation behaviors of $SiO_{1.5}$-hPEA NPs in aqueous solution were investigated under different temperatures, pHs, and ionic strengths. With an increase in temperature, $SiO_{1.5}$-hPEAs NPs aggregate to form large particles due to the destruction of the hydrogen bond between the PEO chain and water at high temperatures. The temperature-dependent size distribution of $SiO_{1.5}$-hPEA particles in aqueous solution was investigated using DLS (Supporting Information Figure S4). Taking $SiO_{1.5}$-hPEA541 NPs as example, its aqueous solution is clear and transparent and the size is about 20 nm in diameter at low temperatures. When heated to 60 °C, the solution became turbid and $SiO_{1.5}$-hPEA541 NPs aggregated into large particles that were several micrometers in diameter. The responsive aggregation behavior of $SiO_{1.5}$-hPEA nanoparticles under different conditions was systematically investigated by recording temperature-dependent transmittance measurements using a UV-vis spectrometer. The corresponding temperature dependence of the transmittance for five aqueous solutions of hybrid nanoparticles is shown in **Figure 2**A; from these, the cloud point (CP) could be obtained. The solutions exhibit sharp transitions from transparent to turbid with the increase in temperature, indicating aggregation of the nanoparticles. At pH 7.0, the CP decreased from $SiO_{1.5}$-hPEA211 to $SiO_{1.5}$-hPEA541-Ac, which could be attributed to the increasing number of hydrophobic moieties.

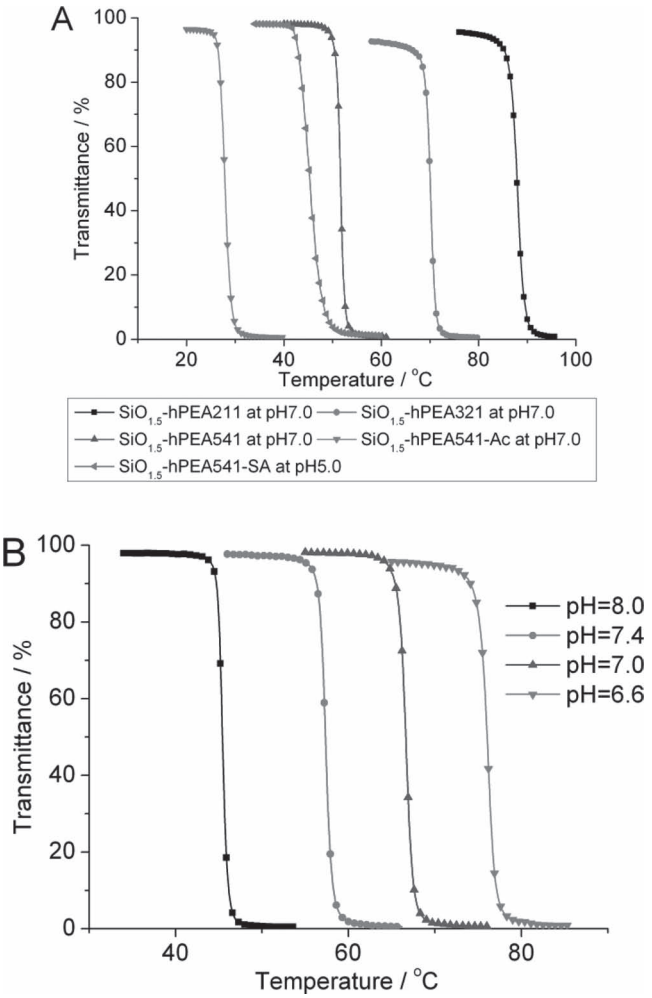

Figure 2. Optical transmittance at 500 nm vs temperature curves for 3 g L^{-1} A) $SiO_{1.5}$-hPEA NPs and B) $SiO_{1.5}$-hPEA541 at different pHs in aqueous solutions.

Due to the tertiary amine moieties in the structure of hybrid nanoparticles, which can be protonated or deprotonated at different pH, $SiO_{1.5}$-hPEA NPs are expected to be responsive to pH. Temperature dependence of the transmittance for $SiO_{1.5}$-hPEA541 aqueous solution at different pH was recorded using UV-vis spectroscopy, the results of which are shown in Figure 2B. When increasing the pH value from 6.6 to 8.0, the CP of $SiO_{1.5}$-hPEA541 decreases from 75.2 to 45.1 °C, indicating that the CP could be controlled by the pH in a wide range. In particular, for $SiO_{1.5}$-hPEA541-SA, the CP first decreases with the increase of pH from 3.2 to 4.6 and then increases at higher pH values (Supporting Information Figure S5). Unlike other $SiO_{1.5}$-hPEA NPs whose CP always decreases with the increase in pH, the special behavior in response to pH could be explained by the zwitterionic structure of $SiO_{1.5}$-hPEA541-SA.[45] The carboxyl groups can be deprotonated at high pH, whereas amino groups become less hydrophilic at this stage (inset of Supporting Information Figure S5B). The ionic strength-responsive properties of $SiO_{1.5}$-hPEA NPs were also investigated using UV-vis spectroscopy (Supporting Information Figure S6). $SiO_{1.5}$-hPEA541

exhibits a very sharp response to ionic strength in aqueous solution. The CP decreases obviously with the increasing NaCl concentration because of the typical salting-out effect.[46]

2.2. Selective Host–Guest Interaction Between $SiO_{1.5}$-hPEA NPs and Hydrophilic Dyes in Water

We studied the adsorption behavior of the five obtained core-crosslinked hybrid $SiO_{1.5}$-hPEA NPs to twelve hydrophilic dyes in water. The structures of these hydrophilic dyes are summarized in **Table 1** and they can be divided into three types: anionic, cationic, and neutral. The adsorption experiments were carried out in a centrifuge tube by precipitation of the dyes along with $SiO_{1.5}$-hPEAs in aqueous solution. Because of their thermal response, $SiO_{1.5}$-hPEA NPs aggregate and precipitate at temperatures higher than the CP. The initial concentration of the dyes was fixed and $SiO_{1.5}$-hPEA NPs was 10 g L^{-1} in all experiments. As shown in **Figure 3**, the UV-vis spectra of $SiO_{1.5}$-hPEA NPs and the dye mixed solution were recorded first. After heating above the CP for 10 min, the turbid solution was centrifuged and the UV-vis spectra of the dyes in the supernatant were also recorded for the determination of dye uptake. It can be readily seen with the naked eye that after heating and centrifugation, most of the Ponceau S (PS) precipitated along with $SiO_{1.5}$-hPEA541 NPs and the supernatant became almost colorless (Figure 3A). The amount of PS in supernatant could be calculated from the corresponding UV-vis spectra (Figure 3C), which indicated ≈2.2% of the initial dye was left in the supernatant. On the contrary, Methylene blue (MB) did not precipitate along with $SiO_{1.5}$-hPEA541 and ≈92.7% of the initial dye was left in the supernatant (Figure 3B,D). The comparison of these two cases indicated that $SiO_{1.5}$-hPEA541 NPs exhibited strong interaction with PS but much weaker interaction with MB. It is important to introduce a parameter to quantitate this host–guest interaction for systematic investigation. We propose a

Table 1. Molecular structures of and abbreviations for the twelve dyes.

Dye	Structure	Dye	Structure
Bordeaux red (BoR)	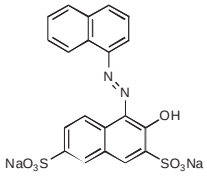	Methyl orange (MO)	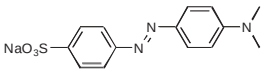
Ponceau S (PS)	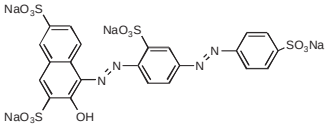	Neutral red (NR)	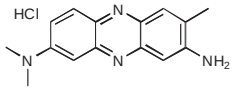
Amido black 10B (10B)	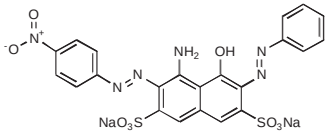	Safranine T (ST)	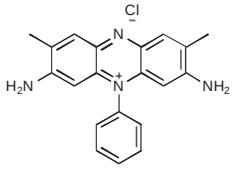
Rose bengal (RB)	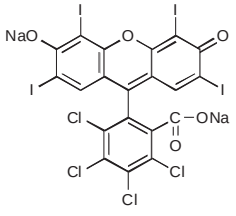	Rhodamine 6G (R6G)	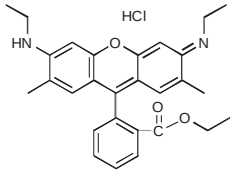
Bismarck brown Y (BY)	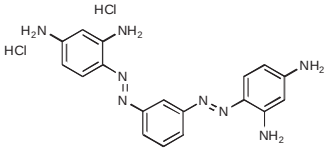	Calcein (Cal)	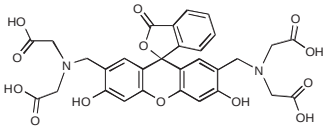
Alizarin yellow R (AYR)	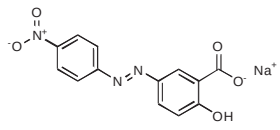	Methylene blue (MB)	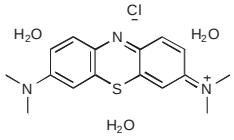

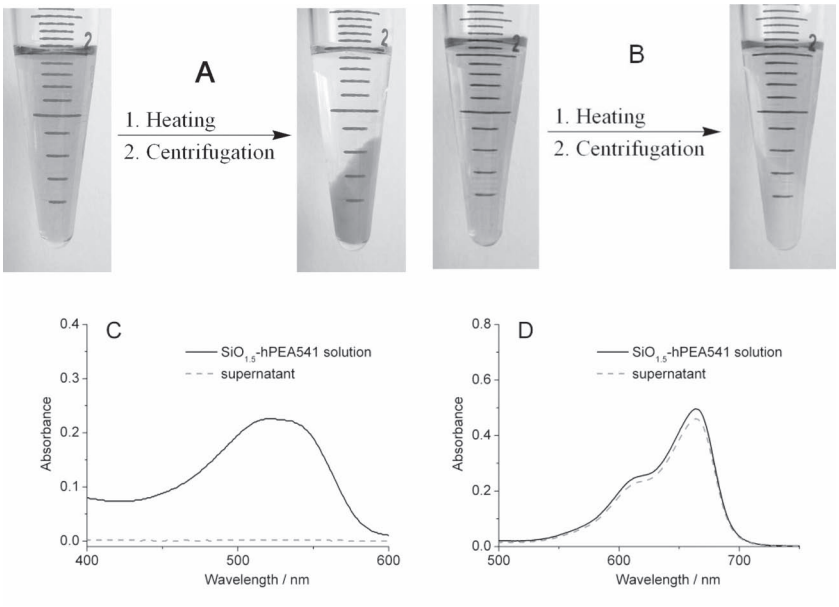

Figure 3. Adsorption experiments of single dye. Photograph of PS (A) and MB (B) precipitated along with $SiO_{1.5}$-hPEA541 after heating and centrifugation. UV-vis spectra of PS (C) and MB (D) during the adsorption experiment.

distribution coefficient (K) for the partitioning of dyes between $SiO_{1.5}$-hPEA NPs and water to define the host–guest interaction; this is shown in Equation (1):

$$K = \frac{[\text{Dye}]_{\text{NP}}}{[\text{Dye}]_{\text{aq}}} \quad (1)$$

where $[\text{Dye}]_{\text{NP}}$ (mmol L^{-1}) is the molar concentration of the dye in the hybrid nanoparticles and $[\text{Dye}]_{\text{aq}}$ (mmol L^{-1}) is the molar concentration of the dye in the aqueous phase.

To confirm that K is a constant or dependent on the initial dye's concentration, we performed a series of adsorption experiments in which the initial concentrations of the dyes were varied from 0.025 to 0.5 mmol L^{-1}. After precipitation along with $SiO_{1.5}$-hPEA NPs in water, the dye concentration versus different initial dye concentration was measured, as shown in **Figure 4**. A linear relationship was observed, independent of the guest dye or host $SiO_{1.5}$-hPEA NPs, suggesting that the distribution equilibrium of dyes between $SiO_{1.5}$-hPEA NPs and aqueous solution could be measured. This is expressed in Equation (2):

$$[\text{Dye}]_{\text{NP}} \times 0.01 + [\text{Dye}]_{\text{aq}} \times 0.99 = [\text{Dye}]_0 \quad (2)$$

where $[\text{Dye}]_0$ (mmol L^{-1}) is the initial dye concentration and $SiO_{1.5}$-hPEA NPs concentration is 10 g L^{-1}, around 1% (wt%) in aqueous solution. Thus the distribution coefficient (K) of each dye could be calculated from the slope of the fit line in Figure 4 ($[\text{Dye}]_0/[\text{Dye}]_{\text{aq}}$) according to combination of Equation (1) and (2)

$$K = \frac{[\text{Dye}]_{\text{NP}}}{[\text{Dye}]_{\text{aq}}} = 100 \times \frac{[\text{Dye}]_0}{[\text{Dye}]_{\text{aq}}} - 99 \quad (3)$$

Taking the linear relationship shown in Figure 4 into consideration, we can conclude that the distribution coefficient (K) is a constant at low concentration of dye, which is independent of the initial dye concentration. According to Equation (3), K for twelve dyes with five $SiO_{1.5}$-hPEA NPs were calculated and the results are summarized in **Table 2**. It is easily seen that K can reflect the strength of the host–guest interaction between $SiO_{1.5}$-hPEA NPs and the dyes: a large value of K indicates a strong host–guest interaction.

2.2.1. Effect of the Molecular Structure of Guest Dyes

According to distribution coefficient (K) shown in Table 2, $SiO_{1.5}$-hPEA NPs exhibit very strong interaction with BoR, PS, 10B, BY, RB, AYR, and MO, but much weaker affinity for R6G, Cal, and MB independent of the charge state of both the $SiO_{1.5}$-hPEA NPs and the dyes. The cationic dye BY shows strong affinity for $SiO_{1.5}$-hPEA NPs, while the anionic dye Cal shows limited affinity to the hosts, which contain amino groups and are expected to be positively charged; this indicates that electrostatic interaction between host nanoparticles and guest dyes is not the predominant factor that determines K. This result is in contrast to that from other reports.[28,34,37,47] If the different dyes with high K are compared it emerges that, except for RB, all dyes (BoR, PS, 10B, BY, AYR, and MO) with a strong interaction with $SiO_{1.5}$-hPEA NPs contain azo moieties regardless of the charges of the dyes. Taking the dye's structure with low K into consideration, we can find that the structure of the dye itself is the key factor determining the host-guest interaction.

To further understand this host–guest interaction, the UV-vis spectra of different dyes with or without $SiO_{1.5}$-hPEA541 NPs were recorded. As shown in **Figure 5**A–C, dyes PS, RB, and MO with high K exhibit an obvious bathochromic shift or hypsochromic shift of absorption maxima (λ_{max}) in the presence of $SiO_{1.5}$-hPEA541 NPs. The shift of λ_{max} should be ascribed to the change in the microenvironment of dyes in aqueous solution. For example, λ_{max} of RB red-shifted from 546 to 561 nm after adding $SiO_{1.5}$-hPEA541 NPs, which is close to the RB absorption in a medium-polar solution of THF (λ_{max} = 562 nm). The significantly red-shifted λ_{max} of RB indicates that RB molecules were sequestered as guests into the hydrophobic core of $SiO_{1.5}$-hPEA541 NPs. The polarity of the nanoparticles' core, composed of PPO chains, is similar to THF. Although RB is hydrophilic, the polarity of RB might be comparable to THF and the core of $SiO_{1.5}$-hPEA541 NPs can thus be encapsulated by $SiO_{1.5}$-hPEA541 NPs. Therefore, the polarity interaction plays an important role in the host–guest interaction between $SiO_{1.5}$-hPEA541 NPs and hydrophilic dyes. Maskos also reported the incorporation of hydrophilic dyes in the interior of poly(organosiloxane) nanoparticles based on polarity interactions other than ionic interactions.[48,49] As shown in Figures 5D–F, in contrast, λ_{max} of dyes such as R6G, Cal, and MB,

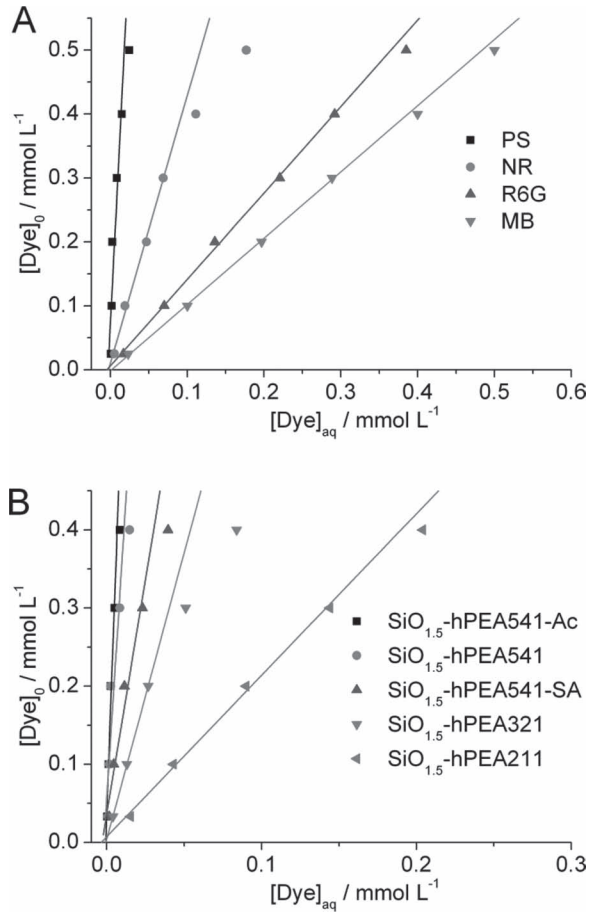

Figure 4. Dispersion of single dye in hybrid NPs and water solution. A) Dye concentration in the supernatant ($[Dye]_{aq}$) under various initial concentrations ($[Dye]_0$) after centrifugation with $SiO_{1.5}$-hPEA541 (c = 10 g L^{-1}). B) PS concentration in the supernatant ($[Dye]_{aq}$) under various initial concentrations ($[Dye]_0$) after centrifugation with different $SiO_{1.5}$-hPEA NPs (c = 10 g L^{-1}). Each plot was determined at the maximum of absorbance of each dye.

all with low K, did not change after adding hybrid NPs, which also demonstrates the limited interaction of dye molecules with the hybrid NPs. Therefore, the dyes showing strong interaction with hybrid NPs (high K) can be encapsulated by $SiO_{1.5}$-hPEA hybrid nanoparticles. The strong host–guest interaction, especially in the case of azo dyes, might be explained mainly by the polarity and topological matching of the guest molecules.[50,51]

2.2.2. Effect of the Structure of Host $SiO_{1.5}$-hPEA NPs

In order to understand the effect of the host structure, five $SiO_{1.5}$-hPEA NPs with different structures were designed and prepared. Comparing the three hosts $SiO_{1.5}$-hPEA211, $SiO_{1.5}$-hPEA321, and $SiO_{1.5}$-hPEA541, we can find that the distribution coefficient (K) of all twelve dyes increases from $SiO_{1.5}$-hPEA211 to $SiO_{1.5}$-hPEA541 (Table 2). The difference in the structure of these three hybrid NPs is the PEO/PPO short chain ratio in backbone. It is obvious that K increases with the increasing number of hydrophobic PPO chains, indicating the hydrophobic cores of $SiO_{1.5}$-hPEA NPs play an important role in the distribution coefficient.

Compared with $SiO_{1.5}$-hPEA541, $SiO_{1.5}$-hPEA541-Ac, which has ester groups, exhibited a higher K for dyes such as PS, 10B, RB, and ST, indicating the more hydrophobic core of NPs leads to higher adsorption efficiency of dyes, which is consistent with the previous result. For some other dyes such as BoR, BY, AYR, MO, and NR, the distribution coefficient decreases slightly, which is probably due to the topological change after esterification of hydroxyl groups. After the introduction of carboxylic groups, $SiO_{1.5}$-hPEA541-SA NPs are expected to be negatively charged. Compared with the positively charged $SiO_{1.5}$-hPEA541, $SiO_{1.5}$-hPEA541-SA exhibited a lower K for the cationic dyes BY, NR, and MB, indicating that electrostatic interaction has no effect on the host–guest interaction, which is in good agreement with the previous discussion. As for dyes with sulfonate or carboxylate groups such as BoR, PS, 10B, RB, MO, and Cal, the K for $SiO_{1.5}$-hPEA541-SA, which has a negative charge, decreases slightly compared to $SiO_{1.5}$-hPEA541; this might be caused by

Table 2. The distribution coefficient ($K = [Dye]_{SiO1.5\text{-}hPEA}/[Dye]_{aq}$) for the partitioning of dyes between $SiO_{1.5}$-hPEA NPs and water.[a)]

Dye	$SiO_{1.5}$-hPEA211	$SiO_{1.5}$-hPEA321	$SiO_{1.5}$-hPEA541	$SiO_{1.5}$-hPEA541-Ac	$SiO_{1.5}$-hPEA541-SA
BoR	267.3	1329.6	4662.9	734.3	1350.3
PS	116.5	707.5	4446.4	16567.7	1941.8
10B	282.7	432.9	3472.4	33234.3	1655.4
RB	734.3	801.9	2282.0	19901.0	636.3
BY	190.0	550.4	1105.8	625.6	999.9
AYR	156.8	714.0	1024.6	256.9	1252.4
MO	198.6	456.6	1024.6	891.1	337.7
NR	91.8	234.3	401.0	307.5	18.5
ST	31	47.2	60.7	67.4	127.8
R6G	27.7	37.8	48.7	34.0	53.2
Cal	7.8	7.4	22.5	14.1	9.2
MB	2.6	8.4	8.9	1.0	7.3

[a)]Concentration of the nanoparticles in water (2 mL): c = 10 g L^{-1}; concentration of the dye in water (2 mL): c = 0.033 mmol L^{-1}. NaCl added and heating temperature for each NPs: $SiO_{1.5}$-hPEA211 (c_{NaCl} = 4 g L^{-1}, temperature T = 90 °C); $SiO_{1.5}$-hPEA321 (c_{NaCl} = 2 g L^{-1}, T = 60 °C); $SiO_{1.5}$-hPEA541 (c_{NaCl} = 2 g L^{-1}, T = 50 °C); $SiO_{1.5}$-hPEA541-SA (c_{NaCl} = 6 g L^{-1}, T = 70 °C). For $SiO_{1.5}$-hPEA541-Ac, buffered solution (phosphate buffered saline (PBS)) at pH 7.0 was used instead of adding NaCl (T = 40 °C).

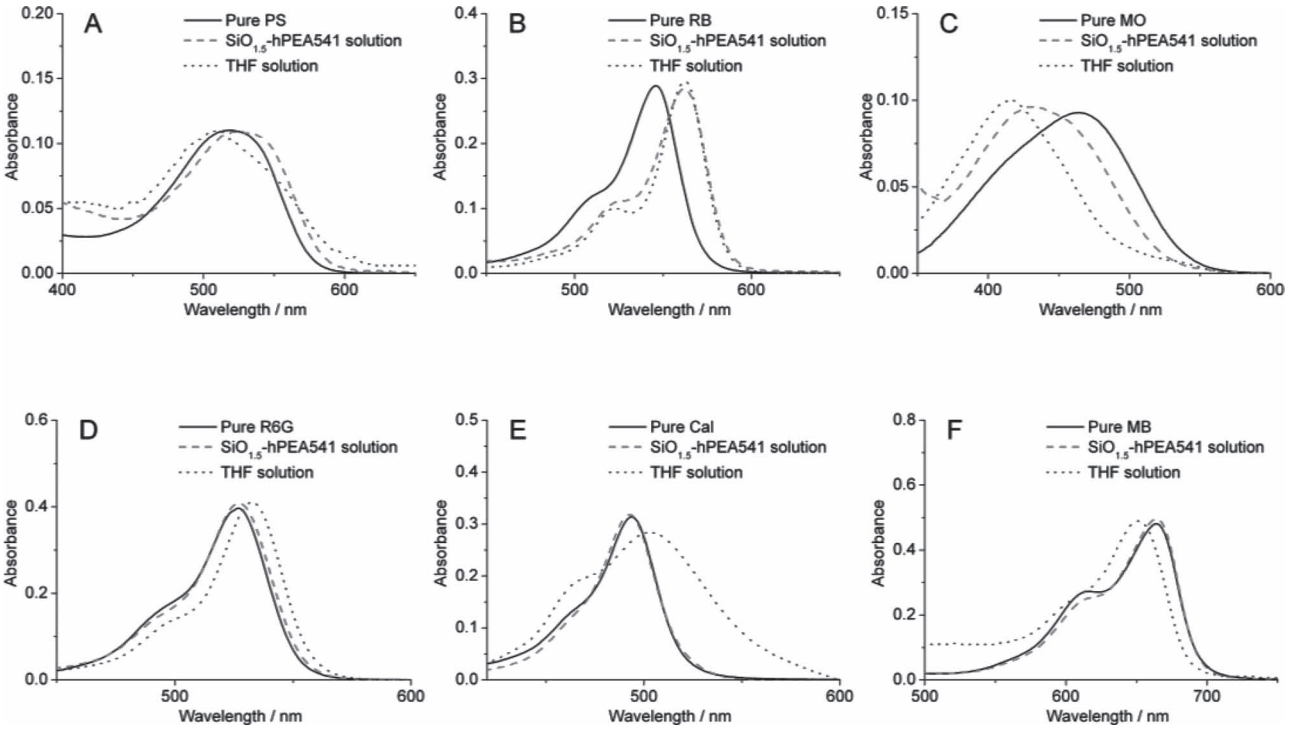

Figure 5. UV-vis spectra of different dyes in pure water (solid line), $SiO_{1.5}$-hPEA541 aqueous solution (dashed line), and THF solution (dotted line). A) PS, B) RB, C) MO, D) R6G, E) Cal, and F) MB.

the decreasing hydrophobicity, not by electrostatic repulsion. In summary, we can conclude that molecular structure of guest dye itself is critical for the selectivity, and the hydrophobicity, not the electrostatic interaction, of the host $SiO_{1.5}$-hPEA NPs plays an important role in the strength of the host–guest interaction.

2.3. Smart Separation of Mixed Dyes

Motivated by the unique selective adsorption of hydrophilic dyes, $SiO_{1.5}$-hPEA NPs are expected to be used in the separation of dye mixture in aqueous solution. Taking the mixture of PS-MB as an example, PS with its high *K* can precipitate along with $SiO_{1.5}$-hPEA NPs from aqueous solution; meanwhile MB, which has a low *K*, is expected to remain in the supernatant after separation (**Scheme 3**). To prove this assumption, different mixtures of dyes were tested in the presence of different $SiO_{1.5}$-hPEA NPs in the separation experiment. Based on the obtained *K*, the concentration of dyes can be calculated in the supernatant after heating and centrifugation using Equation (4):

$$\left.\begin{aligned}\left[Dye1\right]_{aq} &= \frac{100\times\left[Dye1\right]_0}{k_1+99}\\ \left[Dye2\right]_{aq} &= \frac{100\times\left[Dye2\right]_0}{k_2+99}\end{aligned}\right\} \Rightarrow \frac{\left[Dye1\right]_{aq}}{\left[Dye2\right]_{aq}} = \frac{\left[Dye1\right]_0}{\left[Dye2\right]_0}\times\frac{k_2+99}{k_1+99} \quad (4)$$

In Equation (4), the concentration of $SiO_{1.5}$-hPEA NPs should be 1% (by weight) and the mutual interference of two dyes is not taken into consideration. After separation, the concentrations of dyes in the supernatants were determined from the UV-vis spectra. The theoretical and practical values of dye concentration in the supernatant are summarized in **Table 3**. As shown in Table 3 and **Figure 6**, the practical values of the dye concentration are consistent with the theoretical values for all evaluated mixtures of dye, suggesting that Equation (4) can correctly predict the concentration of dye after separation.

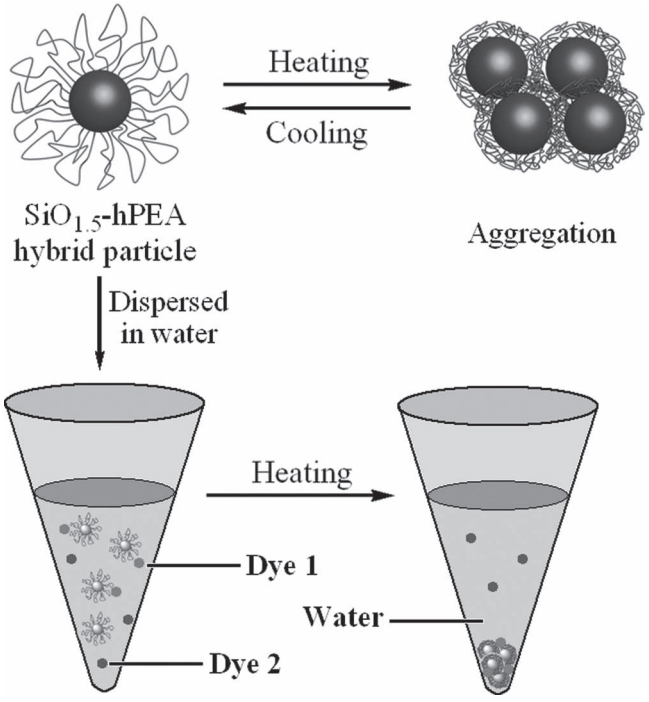

Scheme 3. Mechanisms for the reversible aggregation of $SiO_{1.5}$-hPEA NPs and their applications in the separation of mixture of dyes.

Table 3. Quantification of dye by UV-vis spectroscopy of the supernatant after separation experiment.[a)]

NO	Hybrid NP	Mixed dyes	$[Dye1]_0$ [mmol L^{-1}]	$[Dye2]_0$ [mmol L^{-1}]	Theoretical value			Practical value		
					$[Dye1]_{aq}$ [mmol L^{-1}[	$[Dye2]_{aq}$ [mmol L^{-1}]	$[Dye1]_{aq}/[Dye2]_{aq}$	$[Dye1]_{aq}$ [mmol L^{-1}]	$[Dye2]_{aq}$ [mmol L^{-1}]	$[Dye1]_{aq}/[Dye2]_{aq}$
#1	$SiO_{1.5}$-hPEA321	NR-R6G	0.070	0.164	0.021	0.120	0.175	0.018	0.118	0.152
#2	$SiO_{1.5}$-hPEA321	NR-MB	0.075	0.111	0.023	0.103	0.223	0.024	0.097	0.247
#3	$SiO_{1.5}$-hPEA541	BY-ST	0.086	0.122	0.007	0.076	0.092	0.006	0.075	0.080
#4	$SiO_{1.5}$-hPEA541	NR-R6G	0.082	0.149	0.016	0.101	0.158	0.023	0.111	0.207
#5	$SiO_{1.5}$-hPEA541-Ac	AYR-Cal	0.081	0.134	0.023	0.119	0.193	0.022	0.111	0.198

[a)]Concentration of the nanoparticles in water (2 mL): $c = 10$ g L^{-1}.

Based on Equation (4), the mixture of dyes with different K can be separated in the presence of $SiO_{1.5}$-hPEA NPs. Taking the mixture of PS-MB and $SiO_{1.5}$-hPEA541 NPs as an example ($K_{PS}/K_{MB} = 1393$), the initial concentrations of PS and MB are almost the same. After heating and centrifugation, almost all PS precipitated along with the $SiO_{1.5}$-hPEA541 NPs in the bottom, but most MB remained in the supernatant (**Figure 7**). The concentration of PS and MB in the supernatant was determined using UV-vis spectroscopy (Figure 7B). The concentration of PS in the supernatant decreased from the initial 0.102 mmol L^{-1} to 0.005 mmol L^{-1}, which is about 5% to the concentration of MB (0.101 mmol L^{-1}). In other words, the purity of MB in supernatant is about 95% after one-pot process of separation.

In the case of the mixture of dyes with similar K values, the separation experiment was also tested (**Figure 8**). As shown in Figure 8B, mixed NR-R6G dye solution ($[NR]_0/[R6G]_0 = 0.550$, $K_{NR}/K_{R6G} = 8.23$) were tested using the same method. After a one-pot process, the concentration ratio in the supernatant ($[NR]_{aq}/[R6G]_{aq}$) was reduced to about 0.198, which is close to the theoretical value (0.163). In order to reach a deeper separation, the second stage separation experiment was carried out with the supernatant followed by adding $SiO_{1.5}$-hPEA541 NPs under the same conditions. It was found from the UV-vis spectra (Figure 8C) that after the second stage process, the ratio of $[NR]_{aq}/[R6G]_{aq}$ in supernatant was further reduced to 0.083, which is also comparable to the theoretical value (0.058). Therefore, based on their different K, the mixture of dyes can be separated using a one-pot or a two-pot process.

Finally, the regeneration of the hybrid NPs was investigated. The use of hybrid nanoparticles as recyclable separation agents was demonstrated using dialysis. After dialysis against water

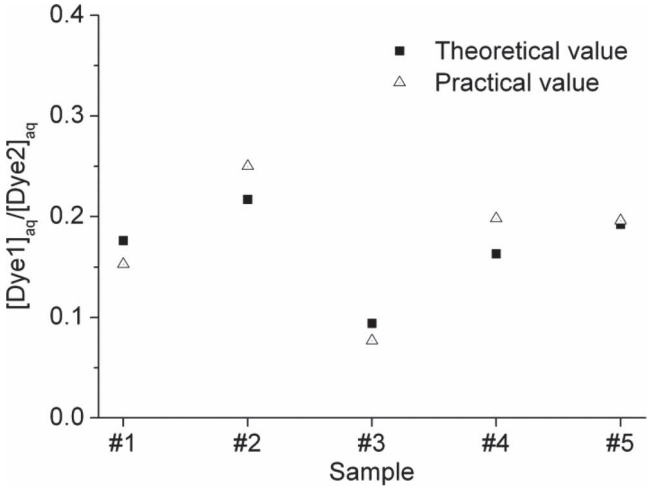

Figure 6. Dye concentration ratio of the mixed dyes in supernatant ($[Dye1]_{aq}/[Dye2]_{aq}$) after separation by using hybrid NPs for five sample experiments. Theoretical values (■) and practical values (△) are compared.

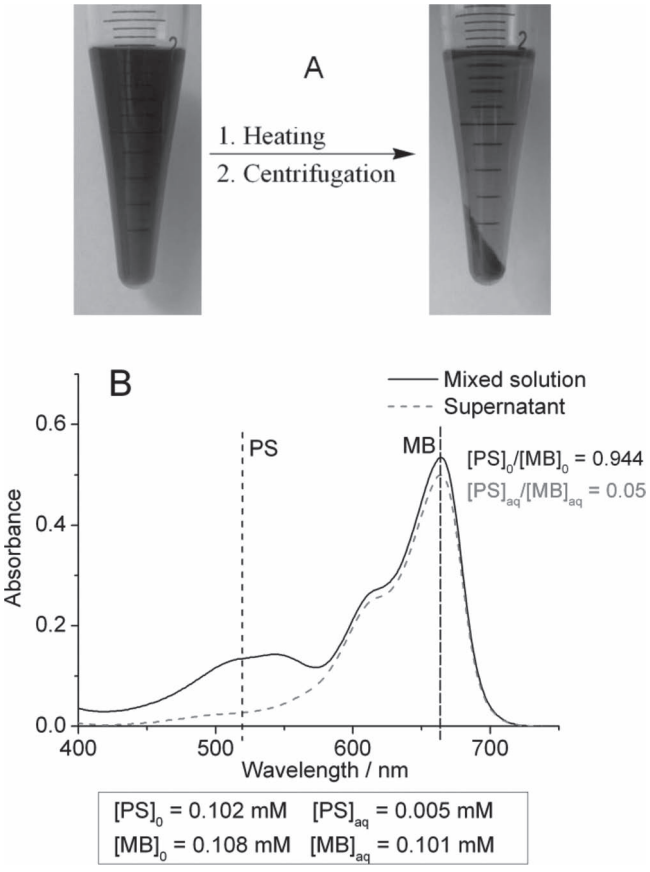

Figure 7. One-pot separation of mixed dyes PS-MB in aqueous solution. A) Photograph of PS-MB separation using $SiO_{1.5}$-hPEA541 after heating and centrifugation. B) UV-vis spectra of PS-MB during the separation experiment.

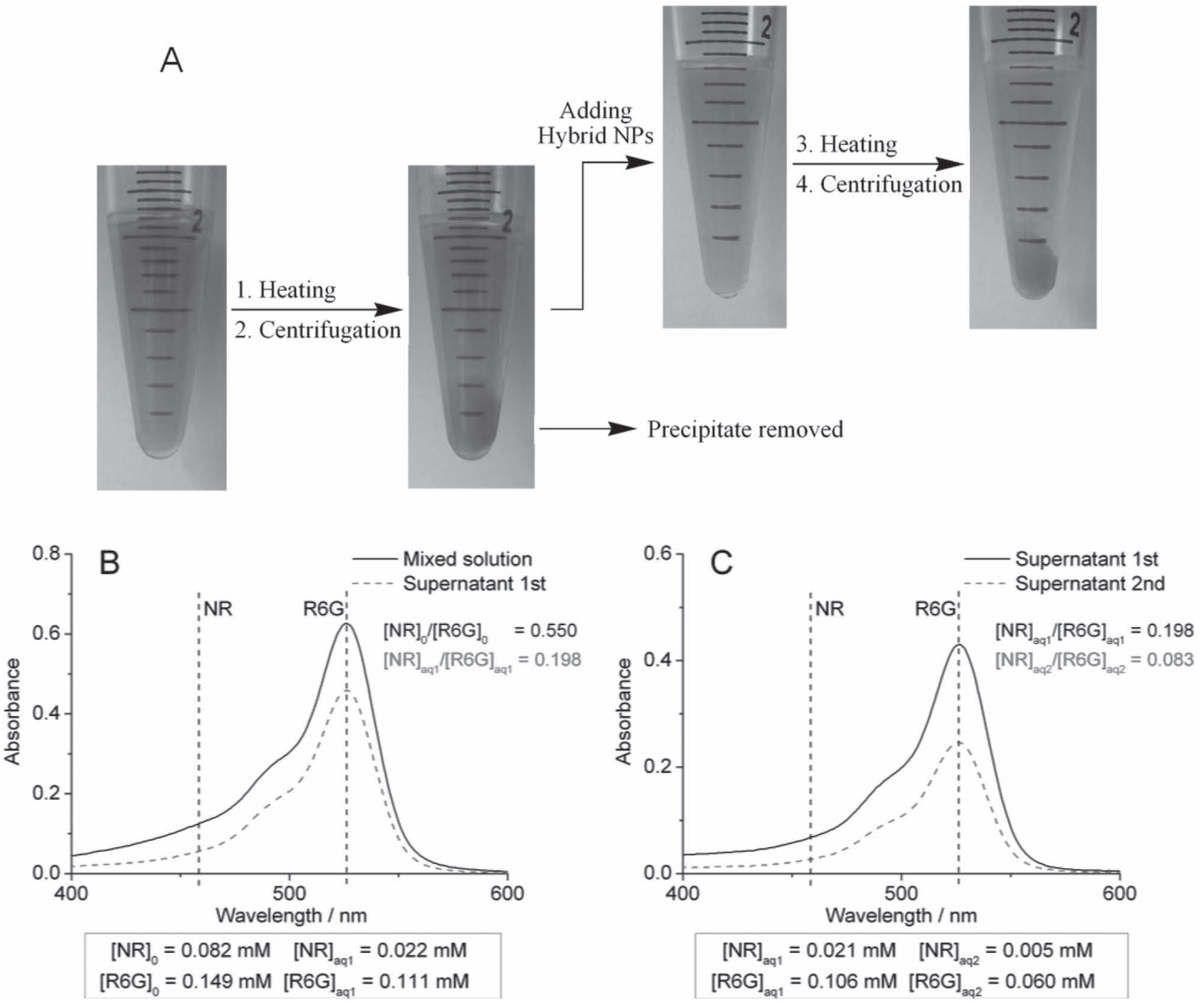

Figure 8. Two-stage separation of mixed dyes NR-R6G in aqueous solution. A) Photograph of the two stage NR-R6G separation process using $SiO_{1.5}$-hPEA541 NPs. UV-vis spectra of NR-R6G in the first stage (B) and second stage (C) separation experiments.

using a cellulose ester dialysis membrane (molecular weight cutoff (MWCO) = 3500), the dyes could be removed and the pure hybrid NPs were obtained (Supporting Information Figure S7). This is environmentally friendly and convenient for the regeneration. In addition, a difference in dialysis time needed for different dye molecules is observed. As for R6G, around 80% of the dyes could be released after 6 h. However, this process is much slower for the release of BoR. It took about 5 days for around 80% of BoR released, which indicates a strong host–guest interaction between BoR and $SiO_{1.5}$-hPEA541 NPs. This result is also in good agreement with their obtained distribution coefficient.

3. Conclusions

In this work, host–guest interactions between various hydrophilic dye molecules and $SiO_{1.5}$-hPEA hybrid nanoparticles in aqueous solution were studied. A series of organosilica hybrid nanoparticles ($SiO_{1.5}$-hPEA NPs) based on hPEA was prepared and their multiresponses to temperature, pH, and ionic strength were demonstrated. $SiO_{1.5}$-hPEA NPs exhibit a host–guest interaction to the guest dyes with different strength. With the increasing hydrophobic PPO chains of the host $SiO_{1.5}$-hPEA NPs, their interaction with guest dyes increases, regardless of the charge states of the dye and $SiO_{1.5}$-hPEA NPs. The electrostatic interaction has a very limited effect on the host–guest interaction. The distribution coefficient ($K = [Dye]_{SiO1.5\text{-}hPEA}/[Dye]_{aq}$) for partitioning of dyes between $SiO_{1.5}$-hPEA NPs and water is proposed to define the strength of the host–guest interaction between the nanoparticles and dyes. $SiO_{1.5}$-hPEA541-Ac NPs exhibit very strong interaction with dye 10B, with a K value of 33 234, which is 3×10^4 times higher than that for MB. The large difference in K indicates that $SiO_{1.5}$-hPEA NPs have a selective interaction with different hydrophilic dyes in aqueous solutions. Based on the established K, we have demonstrated a

methodology for the separation of the different mixture of dyes in water using $SiO_{1.5}$-hPEA NPs. We believe that this fundamental understanding of host–guest interactions is helpful for the design and application of these hybrid nanoparticles, such as in the controlled separation and delivery.

4. Experimental Section

Formation of the Core-Crosslinked Organosilica Hybrid Nanoparticles ($SiO_{1.5}$-hPEA NPs): The synthesis processes for TMS-hPEAs are depicted in Scheme 1. TMS-hPEAs were hydrolyzed and condensed in one pot by direct dispersion in water. The polymer was dispersed in aqueous solution immediately to form a transparent solution with a concentration of 20 g L^{-1}, followed by gradual hydrolysis and condensation of the trimethoxysilyl groups for 3 days to form the core crosslinked hybrid nanoparticles ($SiO_{1.5}$-hPEA NPs).

Adsorption Experiment: An organosilica hybrid NPs solution (20 mg, 1 mL) was added to dye in aqueous solution (0.066 mmol L^{-1}, 1 mL) in a centrifuge tube. The mixed solution was heated above the CP for 10 min to ensure full separation of two phases. Then the turbid solution was centrifuged at 2000 rpm for 2 min. During the process, the UV-vis spectra of the dye in the initial aqueous solution with or without hybrid NPs, as well as in supernatant after centrifugation, were recorded with a UV-2550 spectrophotometer (Shimadzu, Japan, [Dye] = 6.6×10^{-6} M). In the experiment for each hybrid NP, a small amount of NaCl (≈2–6 g L^{-1}) were added to tune the CP; $SiO_{1.5}$-hPEA541-Ac was in PBS solution at pH 7.0. The absorption coefficient could be obtained from calibration curves of each dye in aqueous solution, so the dye concentration was calculated from the absorbance at maximum absorption wavelength (λ_{max}).

Characterization: ^{1}H NMR measurements were carried out using a Varian Mercury Plus spectrometer, operating at 400 MHz and using $CDCl_3$ as the solvent and tetramethylsilane as an internal standard. FTIR spectra of the products were recorded on a Perkin-Elmer Paragon1000 FTIR spectrometer. TEM measurements were carried out using a JEOL JEM-2100 microscope, operating at 200 kV. A drop of 1 g L^{-1} $SiO_{1.5}$-hPEA NPs aqueous solution was placed onto a copper grid and the excess solution was removed by a filter paper.

UV-vis spectra of samples in aqueous solution were recorded to determine the CP of the polymers. The optical transmittance of the $SiO_{1.5}$-hPEA NPs solutions (concentration was 3 g L^{-1}) was measured at 500 nm with a UV-2550 spectrophotometer (Shimadzu, Japan) equipped with a thermo cell at a heating rate of 1 °C min^{-1}. The temperature at 80% light transmittance of the polymer solution was defined as the CP.

DLS measurements were performed in $SiO_{1.5}$-hPEA NPs solutions (concentration was 1 g L^{-1}) using a Zetasizer Nano ZS90 instrument (Malvern Instruments) equipped with a 4 mW He-Ne laser ($\lambda = 633$ nm) at an angle of 90°, an avalanche photodiode detector with high quantum efficiency, and an ALV/LSE-5003 multiple τ digital correlator electronics system. A regularized Laplace inversion (CONTIN algorithm) was applied to analyze the obtained autocorrelation functions. The size of the nanoparticles was determined using the volume-weighted distribution of particle sizes.

Supporting Information

Supporting Information is available from the Wiley Online Library or from the author.

Acknowledgements

The authors thank the National Nature Science Foundation of China (21174085), Science & Technology and Education Commission of Shanghai Municipal Government (11QA1403100, 12ZZ020), and the Shanghai Leading Academic Discipline Project (B202) for their financial support. X.S.J. is supported by the SMC Project of Shanghai Jiao Tong University.

Received: November 30, 2011
Revised: January 17, 2012
Published online: April 5, 2012

[1] J. Han, C. Gao, *Curr. Org. Chem.* **2011**, *15*, 2.
[2] C. H. Liu, C. Gao, D. Y. Yan, *Macromolecules* **2006**, *39*, 8102.
[3] T. Miyagawa, M. Yamamoto, R. Muraki, H. Onouchi, E. Yashima, *J. Am. Chem. Soc.* **2007**, *129*, 3676.
[4] Y. Lin, X. H. Liu, Z. M. Dong, B. X. Li, X. S. Chen, Y. S. Li, *Biomacromolecules* **2008**, *9*, 2629.
[5] M. J. Liu, K. Kono, J. M. J. Frechet, *J. Control. Release* **2000**, *65*, 121.
[6] C. Kojima, K. Kono, K. Maruyama, T. Takagishi, *Bioconjugate Chem.* **2000**, *11*, 910.
[7] G. Chen, Z. Guan, *J. Am. Chem. Soc.* **2004**, *126*, 2662.
[8] Y. Chen, C. M. Dong, *J. Phys. Chem. B* **2010**, *114*, 7461.
[9] S. Xu, Y. Luo, R. Haag, *Macromol. Biosci.* **2007**, *7*, 968.
[10] J. F. G. A. Jansen, E. W. Meijer, E. M. M. de Brabander-van den Berg, *J. Am. Chem. Soc.* **1995**, *117*, 4417.
[11] M. Kramer, J. F. Stumbe, H. Turk, S. Krause, A. Komp, L. Delineau, S. Prokhorova, H. Kautz, R. Haag, *Angew. Chem. Int. Ed.* **2002**, *41*, 4252.
[12] C. J. Jang, J. H. Ryu, J. D. Lee, D. Sohn, M. Lee, *Chem. Mater.* **2004**, *16*, 4226.
[13] H. Frey, S. E. Stiriba, H. Kautz, *J. Am. Chem. Soc.* **2002**, *124*, 9698.
[14] S. K. Ghosh, S. Kawaguchi, Y. Jinbo, Y. Izumi, K. Yamaguchi, T. Taniguchi, K. Nagai, K. Koyama, *Macromolecules* **2003**, *36*, 9162.
[15] D. Parasuraman, M. J. Serpe, *ACS Appl. Mater. Interface* **2011**, *3*, 2732.
[16] M. M. Mohamed, *J. Colloid Interface Sci.* **2004**, *272*, 28.
[17] Y. R. Wang, W. Chu, *Ind. Eng. Chem. Res.* **2011**, *50*, 8734.
[18] Y. C. Sharma, Uma, A. S. K. Sinha, S. N. Upadhyay, *J. Chem. Eng. Data* **2010**, *55*, 2662.
[19] V. E. Campbell, P. A. Chiarelli, S. Kaur, M. S. Johal, *Chem. Mater.* **2005**, *17*, 186.
[20] G. Crini, H. N. Peindy, F. Gimbert, C. Robert, *Sep. Purif. Technol.* **2007**, *53*, 97.
[21] W. Tanthapanichakoon, P. Ariyadejwanich, P. Japthong, K. Nakagawa, S. R. Mukai, H. Tamon, *Water Res.* **2005**, *39*, 1347.
[22] X. Zhuang, Y. Wan, C. M. Feng, Y. Shen, D. Y. Zhao, *Chem. Mater.* **2009**, *21*, 706.
[23] C. H. Weng, Y. T. Lin, T. W. Tzeng, *J. Hazard Mater.* **2009**, *170*, 417.
[24] A. C. Ueda, L. H. de Oliveira, N. Hioka, M. Aznar, *J. Chem. Eng. Data* **2011**, *56*, 652.
[25] A. Sunder, M. Kramer, R. Hanselmann, R. Mulhaupt, H. Frey, *Angew. Chem. Int. Ed.* **1999**, *38*, 3552.
[26] D. Wilms, S. E. Stiriba, H. Frey, *Acc. Chem. Res.* **2010**, *43*, 129.
[27] Y. Chen, Z. Shen, L. Pastor-Perez, H. Frey, S. E. Stiriba, *Macromolecules* **2005**, *38*, 227.
[28] H. J. Liu, Y. Chen, D. D. Zhu, Z. Shen, S. E. Stiriba, *React. Funct. Polym.* **2007**, *67*, 383.
[29] H. Y. Tian, X. S. Chen, H. Lin, C. Deng, P. B. Zhang, Y. Wei, X. B. Jing, *Chem.-Eur. J.* **2006**, *12*, 4305.
[30] M. Kramer, M. Kopaczynska, S. Krause, R. Haag, *J. Polym. Sci. Polym. Chem.* **2007**, *45*, 2287.
[31] D. C. Wan, H. T. Pu, M. Jin, *Macromolecules* **2010**, *43*, 3809.
[32] D. C. Wan, H. T. Pu, X. Y. Cai, *Macromolecules* **2008**, *41*, 7787.
[33] E. Burakowska, J. R. Quinn, S. C. Zimmerman, R. Haag, *J. Am. Chem. Soc.* **2009**, *131*, 10574.

[34] S. Basu, D. R. Vutukuri, S. Thayumanavan, *J. Am. Chem. Soc.* **2005**, *127*, 16794.
[35] A. Gomez-Escudero, M. A. Azagarsamy, N. Theddu, R. W. Vachet, S. Thayumanavan, *J. Am. Chem. Soc.* **2008**, *130*, 11156.
[36] D. C. Gonzalez, E. N. Savariar, S. Thayumanavan, *J. Am. Chem. Soc.* **2009**, *131*, 7708.
[37] T. S. Kale, A. Klaikherd, B. Popere, S. Thayumanavan, *Langmuir* **2009**, *25*, 9660.
[38] R. Wang, X. S. Jiang, C. F. Di, L. Yin, *Macromolecules* **2010**, *43*, 10628.
[39] R. McHale, N. Ghasdian, N. S. Hondow, P. M. Richardson, A. M. Voice, R. Brydson, X. S. Wang, *Macromolecules* **2010**, *43*, 6343.
[40] S. E. Stiriba, H. Kautz, H. Frey, *J. Am. Chem. Soc.* **2002**, *124*, 9698.
[41] Y. Zhou, W. Huang, J. Liu, X. Zhu, D. Yan, *Adv. Mater.* **2010**, *22*, 4567.
[42] Y. Shen, M. Kuang, Z. Shen, J. Nieberle, H. Duan, H. Frey, *Angew. Chem. Int. Ed.* **2008**, *47*, 2227.
[43] B. Yu, X. S. Jiang, G. L. Yin, J. Yin, *J. Polym. Sci. Polym. Chem.* **2010**, *48*, 4252.
[44] R. K. O'Reilly, C. J. Hawker, K. L. Wooley, *Chem. Soc. Rev.* **2006**, *35*, 1068.
[45] X. S. Jiang, C. F. Di, B. Yu, J. Yin, *ACS Appl. Mater. Interface* **2011**, *3*, 1749.
[46] K. Van Durme, H. Rahier, B. Van Mele, *Macromolecules* **2005**, *38*, 10155.
[47] A. W. Kleij, R. van de Coevering, R. J. M. K. Gebbink, A. M. Noordman, A. L. Spek, G. van Koten, *Chem.-Eur. J.* **2001**, *7*, 181.
[48] N. Jungmann, M. Schmidt, J. Ebenhoch, J. Weis, M. Maskos, *Angew. Chem. Int. Ed.* **2003**, *42*, 1714.
[49] M. Gross, M. Maskos, *Polymer* **2005**, *46*, 3329.
[50] M. W. P. L. Baars, P. E. Froehling, E. W. Meijer, *Chem. Commun.* **1997**, 1959.
[51] S. F. Chen, Q. M. Yu, L. Y. Li, C. L. Boozer, J. Homola, S. S. Yee, S. Y. Jiang, *J. Am. Chem. Soc.* **2002**, *124*, 3395.